



Evaluation of FBMC/OQAM performance using Hybrid MGDFT and PTS approaches in terms of BER, Spectral Efficiency, and PAPR

N Sivapriya ^a, Karthik Kumar Vaigandla ^{b,*}, R Mohandas ^c, Kirubasankar K ^c

^a Department of Computer Application, Cauvery College for Women, Trichy, Tamil Nadu, India

^b Electronics and Communication Engineering, Balaji Institute of Technology and Science, Telangana, India

^c Electronics and Communication Engineering, Chennai Institute of Technology, Chennai, Tamil Nadu, India

* Corresponding Author Email: vkvaigandla@gmail.com

DOI: <https://doi.org/10.54392/irjmt25313>

Received: 07-12-2024; Revised: 17-04-2025; Accepted: 22-04-2025; Published: 05-05-2025



Abstract: The fast advancement of next-generation wireless communication systems requires effective multicarrier transmission methods that improve performance metrics, including Bit Error Rate (BER), Peak-to-Average Power Ratio (PAPR), and Spectral Efficiency (SE). Filter Bank Multicarrier with Offset Quadrature Amplitude Modulation (FBMC/OQAM) has emerged as a promising contender for 6G systems due to its enhanced SE and resilience to frequency selectivity. Nonetheless, the elevated PAPR and BER in FBMC/OQAM systems persist as significant challenges. This paper proposes a hybrid strategy that integrates the Modified Generalized Discrete Fourier Transform Spreading (MGDFTS) technology with the Partial Transmit Sequence (PTS) scheme to improve the performance of FBMC/OQAM systems. The merged operation of MGDFTS and PTS not only minimizes PAPR but also enhances the performance of BER and spectrum efficiency. We thoroughly assess the proposed hybrid model via extensive simulations and performance evaluations, comparing it with traditional FBMC/OQAM systems and recent optimization methods. Simulation findings indicate that the proposed hybrid MGDFTS-PTS method significantly decreases PAPR while preserving a low BER and enhancing SE. This study highlights the promise of the hybrid approach as an acceptable choice for advanced multicarrier communication systems, aiding in the advancement of high-performance 6G networks.

Keywords: BER, DFT, FBMC/OQAM, PAPR, PTS, Spectral Efficiency

1. Introduction

Wireless communications refer to transmitting data between devices that are working on a common electromagnetic spectrum without any physical connectivity. High data rates, low latency, and reliable connectivity become crucial demands in the modern wireless systems as an increase in the demand of data-intensive applications like video streaming, game, and IoT. Techniques of MCM turn out to be of pivotal importance in attaining this end. An advanced MCM scheme, with which OQAM is also associated, is FBMC. This has many advantages over the traditional schemes like OFDM. In FBMC, the available bandwidth is divided into several narrowband subcarriers they carry data independently. The OQAM further improves the time-frequency localization of the subcarriers by transmitting the real and imaginary parts of symbols with a time offset. Together, FBMC/OQAM increases spectral efficiency and diminishes out-of-band emissions; therefore, it is the optimal candidate for next-generation wireless systems. Due to its suitability in addressing ultra-dense network challenges, massive IoT

connectivity, and highly dynamic spectrum environments, FBMC/OQAM is considered for 6G and beyond. Although OFDM dominates in 4G and 5G, this drift toward FBMC/OQAM signals a step ahead in enhancing the efficiency and adaptability of wireless communication.

The multicarrier technology is vastly employed in the present wireless communication (WC) systems, for example, 5G [1]. Of late, much importance has been placed on the investigation of the FBMC technique in association with OQAM in a number of research studies. The technology for 5G, namely (OFDM), has an alternative approach [2-3]. FBMC/OQAM can mitigate some disadvantages of OFDM, such as the need for a cyclic prefix, thereby offering some benefits. The FBMC/OQAM system uses an IFFT and FFT-based filter bank to perform TFL pulse shaping. In addition, the OQAM symbols are interleaved across subcarriers. In comparison, the complexity of the FBMC/OQAM modulation is relatively higher than that of the CP-OFDM modulation scheme. With this technology, OoB emissions can be minimized along with SE enhancement. FBMC/OQAM is one of the MCM

technologies that is reported to be associated with a high level of PAPR problem [4]. In order to improve the performance of FBMC/OQAM, it is important to reduce PAPR. For the last decade, there have been many researchers who presented different techniques to reduce PAPR. Some of them are DFTS, clipping and filtering, PTS, active constellation extension (ACE), tone reservation (TR), selective mapping (SLM), etc. [5]. While these methods significantly reduce PAPR, they are accompanied by drawbacks such as high CC, decreased SE, and an increased BER. The OFDM and FBMC/OQAM share similarities but also have differences. The OFDM signals operate in isolation, while the FBMC/OQAM signals overlap with the next data block signal. The conventional implementation of OFDM methods is not efficient for FBMC/OQAM [6].

The main objectives of the research are:

- i. To evaluate the performance limitations of traditional FBMC/OQAM systems, with a particular focus on BER, PAPR, and SE.
- ii. To formulate a hybrid approach by integrating MGDFTS with PTS to mitigate the issues of high PAPR and BER in FBMC/OQAM systems.
- iii. To evaluate the efficiency of the proposed hybrid MGDFTS-PTS method via extensive simulations and performance evaluation.

2. Literature Review

In the past few days, there has been very good amounts of scholars research done regarding the effective PAPR reduction techniques for the study of FBMC/OQAM systems. The TR approach works by assigning a limited number of tones and sub-ordinately including that within the FBMC transmitted signal. The combination has to be done by this signal in such a manner as to minimize amplitude levels on the peaks. The SW-TR technique efficiently reduces the amplitude peaks demonstrated by the transmitted FBMC signals within the allocated window. The presence of reserved tones and the requirement for many iterations to reduce PAPR lead to a reduction in bandwidth efficiency [7]. The clipping and filtering technique reduces the amplitude of the transmitted signal to an extent that is to some predefined value, so decreasing PAPR, yet it escalates distortion at the receiver side as there exists clipping noise in that context [8]. Both PTS and SLM methods are implemented for FBMC system for PAPR problem elimination. This is achieved by the analysis of the jointly optimum configurations over many FBMC symbols. However, the reduction in PAPR is achieved by introducing more complexity and reducing the data rate, which is contributed due to the use of SI [9]. In the work presented in reference [10], a SLM technique with multiple blocks was proposed. The authors have introduced a TSLM technique in their previous work [11], where an attempt was made to minimize latency by

designing the technique. In a study in [12], there has been a proposed TSLM method that achieves half reduction of complexity. The methods as mentioned above based on the technique of SLM are aware of the properties of overlap between FBMC/OQAM symbols and outperform the conventional techniques of methods in SLM-based. For the reduction of PAPR of FBMC/OQAM signals, another alternative signaling scheme was proposed in reference [13] by generating other signals. The technique involved the analysis of overlapping data blocks for the determination of an appropriate phase rotation sequence (PFS). A segmental PTS referred to in the authors' work in reference [14], has been proposed for subdividing the overlapping FBMC/OQAM signals into numerous segments. An optimization-based technique by the authors in reference [15] made use of an optimization-based segment. The improved S-PTS technique reduces the PAPR of every block of data first, followed by the optimisation of each segment as done at the previous step. The simulations that are demonstrated with both the modified PAPR-based techniques significantly reduce the PAPR of the FBMC/OQAM signal. A multi-block tone reservation method is presented in reference [16]. OFDM vs FBMC has been presented in reference [17]. The authors have proposed methodology for adding neighboring data blocks for optimizing the clipping noise quality. Here the authors have been proposed new approach on FBMC/OQAM with a view of having minimum PAPR without PAPR reduction techniques as said in [18]. Hybrid algorithm was proposed in [19], combining the rules of SLM and TR algorithms. In reference [20] authors used TR and companding techniques to reduce PAPR. Hybrid techniques can potentially perform better in terms of PAPR reduction compared to standalone techniques. In a recent work [21], an approach that was presented on hybrid PAPR minimization was introduced. The technique combines multi-data PTS with TR-based strategies. In the work by [22], a new approach including integration of an enhanced bilayer PTS and clipping-filtering mechanism was proposed. The DFTS technique is highly renowned for the PAPR reduction of an OFDM system. So it can be effectively used in uplink application with minimum power consumption. However, in this case, it has not been enhanced in FBMC systems. Most of the research works are based on DFTS for the enhancement of the effect to reduce PAPR in FBMC systems. Various techniques have been discussed and proposed such as pruned DFT, generalized DFTS (GDFT), identically time-shifted multicarrier (ITSM) condition, and pre-coding technique. The technique that was proposed by the authors in reference [23] was based on pruned DFTS, which reduced both PAPR and CC. The aim of this research work is to minimize PAPR in FBMC/OQAM.

In [24], an approach was proposed to minimize complexity by limiting the number of phase factors. The

stage factors are assigned to each information block to reduce the PAPR of the information blocks. All data blocks are divided into portions, with one data block selected to optimize per area. Another clipping method is employed to further reduce PAPR. The truncated signal is then restored by compressed detection, which prevents a substantial deterioration of the BER at the receiving end. Despite the added complexity from reconstruction processing for the recipient, the total complexity of the system remains lower, accompanied by an enhancement in the spectral efficiency of the conventional system. In [25], four PAPR reduction strategies were developed by adapting the Active Constellation Extension (ACE) method utilized in OFDM systems. The strategies suggested by the authors use the overlapping characteristics of the FBMC symbols. The approaches are categorized into two unique groups: an integrated ACE class and an optimization group. The optimization-based methods enhance a collection of constraints. The interconnected ACE integrates an optimization approach with an adaption of the Smart Gradient - Project (SGP) ACE. The ACE approach is an iterative procedure that considers complexity constraints, necessitating a reduction in repetitions to attain a viable PAPR. The proposed methods seek to minimize overall system complexity by attaining significant PAPR reduction in a single effort. The Artificial Bee Colony (ABC) optimization method, aimed at minimizing the substantial Peak-to-Average Power Ratio (PAPR) for each linked symbol by the use of the minimal combination of optimal phase variables, is suggested in [26]. The model findings indicate that the hybrid SLM-PTS with ABC phase optimization approach may significantly reduce the PAPR with little computing complexity. A solution to address the significant PAPR issue, provided in many forms, is detailed in [27]. The Trellis-based Dispersive-SLM (TDSLIM) approach is introduced to significantly improve PAPR reduction efficiency. To get diminished computational complexity, the authors introduce the TDSLIM technique using ABC phase optimization. A hybrid approach using traditional PTS. The ideal arrangement of phase factors is determined using a movement approach, which has an average computational complexity as outlined in [28]. The paper introduces PTS-based discrete particle swarm optimization (DPSO) with a threshold (PTS-DPSO-TH). To reduce the PAPR value of the transmitted signal, PTS-DPSO-TH employs DPSO to identify the best combination of phase factors. A minimal threshold value is implemented to diminish the frequency of repeats and mitigate the algorithm's complexity. The Continuous-Unconstrained Particle Swarm Optimisation based PTS (CUPSO-PTS) technique is introduced as a novel strategy for choosing appropriate phase rotation factors in [29]. A series of continuous-phase PTS algorithms has been proposed to determine the global optimal phase factor, with mathematical constraints identified inside the continuous-unconstrained search duration. Conversely, a similar unrestricted PTS

optimization may considerably accelerate integration and diminish the total computational expense when the phase aspect values are in the continuous-unconstrained domain. In [30], the Genetic Algorithm - Bilayer Partial Transmit Sequence (GA-BPTS) technique was devised for the reduction of PAPR in FBMC/OQAM systems. The BPTS architecture is analyzed for insufficient phase factors using an advantageous model filter and GA approach. The modeling findings indicate that an FBMC/OQAM system utilizing the GA-BPTS framework may achieve significantly reduced computational costs and improved PAPR reduction compared to conventional methods.

A PSO-Joint PTS (PSO-JPTS) framework, integrating the PSO technique with joint PTS, is established in [31]. Improving the PAPR through JPTS is crucial, and the PAPR optimization system employs the PSO method to reduce computational complexity. The findings indicate that the proposed PSO-based JPTS system markedly reduced the PAPR values while requiring less computational power to analyze the FBMC/OQAM signal. In [32], a Dual Symbol Optimization (DSO) based PTS approach is presented, which independently optimizes neighboring symbols and seeks the most efficient information block with the minimal PAPR by evaluating two adjacent symbols together. In [33], a new combination is presented that employs Repeated Clipping and Filtering (RCF) with different companding algorithms within an FBMC/OQAM framework utilizing MIMO. The optimal outcomes for BER, spectral efficiency, and PAPR reduction are achieved with the combination of RCF and μ -Law. When comparing the modeling results to the unique signal without the removal approach, the PAPR is significantly lowered.

In [34], an approach termed TR and clipping was developed to mitigate PAPR by constraining the signal's excessive amplitude to a predetermined threshold. However, the approaches generate considerable noise outside the zone and significant distortion within the band.

This paper introduces a new scheme for PAPR minimization in FBMC/OQAM systems. This solution strategy is based on the combination of DFTS with PTS technique. The PTS technique involves partitioning and searching between the real and imaginary FBMC/OQAM in order to find the optimal candidate with the minimum PAPR. Besides, the PAPR for each component is determined based on an existing overlapping level between the preceding symbol components. This paper demonstrates that the proposed method significantly improves the PAPR reduction for FBMC/OQAM systems. Table 1 represents the comparisons between PTS and DFT-Spreading (DFT-S).

Table 1. PTS vs DFT-S

Aspect	PTS	DFT-Spreading (DFT-S)
Purpose	Primarily used to reduce PAPR in multicarrier systems like OFDM.	Reduces PAPR and acts as a pre-coding technique in Single Carrier FDMA (SC-FDMA).
Technique Type	PAPR reduction technique.	Signal spreading and pre-coding technique.
PAPR Reduction Mechanism	Divides the signal into sub-blocks and applies phase optimization to minimize PAPR.	Spreads data symbols over multiple subcarriers to create a single-carrier-like waveform.
Application	Common in OFDM-based systems where PAPR is a concern (e.g., LTE, WiMAX).	Used in uplink of LTE (SC-FDMA) to maintain low PAPR and efficient power utilization.
Computational Complexity	High due to exhaustive search for phase factors, especially in exhaustive PTS.	Moderate; involves FFT and IFFT operations for signal spreading.
Spectral Efficiency	Retains spectral efficiency of the multicarrier system.	Retains spectral efficiency while introducing single-carrier-like characteristics.
Power Amplifier Efficiency	Improves due to reduced PAPR, but not as significant as DFT-S.	Significantly improves power amplifier efficiency due to lower PAPR.
Flexibility	Flexible; can be tailored for different sub-block partitioning schemes and phase factor optimization.	Limited to predefined DFT operations.
Implementation Complexity	Higher due to sub-block partitioning and phase optimization.	Simpler to implement compared to PTS.
Processing Delay	Higher because of iterative phase optimization.	Lower delay as it involves linear processing (FFT/IFFT).
Usage in Standards	Widely used in OFDM systems for PAPR reduction.	Adopted in LTE uplink (SC-FDMA).
Performance in Frequency-Selective Channels	Performs well but does not inherently mitigate channel distortion.	Superior performance due to single-carrier-like robustness.

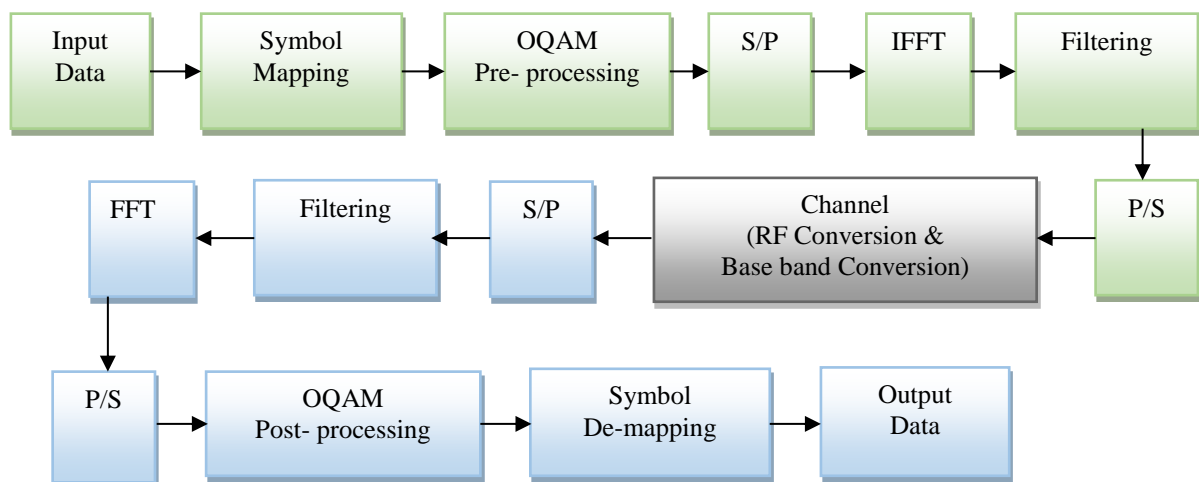


Figure 1. FBMC/OQAM System

3. SYSTEM MODEL

3.1 FBMC/OQAM System

FBMC/OQAM is a sophisticated multicarrier modulation scheme. It achieves high spectral efficiency and low Out-of-Band (OoB) emissions, making it suitable for modern communication systems. The system starts with a stream of input data bits, which are then grouped into symbols for transmission. The input serial data is divided into multiple parallel streams. Each parallel stream corresponds to one subcarrier in the multicarrier system. Each data symbol in the parallel streams is mapped to a constellation point using QAM. These symbols are complex-valued, representing both in-phase (I) and quadrature-phase (Q) components. To improve the spectral efficiency, the real and imaginary parts of the QAM symbols are transmitted at different time instances (offset by half a symbol duration). This creates an effective overlapping structure while avoiding ISI. A synthesis filter bank processes the OQAM symbols. Each subcarrier is filtered using a prototype filter designed to minimize spectral leakage. These filters are implemented efficiently using a polyphase structure, ensuring precise shaping of each subcarrier signal. Each filtered symbol is modulated onto a unique subcarrier frequency. Unlike OFDM, FBMC avoids using a cyclic prefix, which saves bandwidth. The subcarriers, now containing OQAM-modulated data, are combined into a single time-domain signal for transmission. The time-domain signal is transmitted over the communication channel. FBMC's well-localized subcarriers ensure minimal interference between adjacent channels and better performance in frequency-selective channels. At receiver side, the reverse process is applied. The signal is passed through an analysis filter bank to demodulate the subcarriers. OQAM is used to reconstruct the original QAM symbols. Finally, the parallel data streams are converted back to a serial data stream. The basic block diagram of FBMC/OQAM system is shown in figure 1.

Figure 2 depicts the block diagram of the FBMC/OQAM transmitter. OFDM necessitates the use of a CP procedure. In the context of FBMC/OQAM, the use of pulse shaping filter bank (PSFB) and OQAM is necessary in lieu of CP. The input data undergoes modulation using OQAM. The real and imaginary components of each symbol are transferred to subcarriers following the process of serial to parallel conversion. The transmission data block of FBMC/OQAM may be acquired by combining all subcarrier signals after undergoing PF and phase modulation [36]. The signal in the time domain for FBMC/OQAM is represented in equation (1),

$$x(t) = \sum_{p=0}^{N_s-1} \sum_{q=0}^{N_d-1} D_{p,q} g(t) \text{ for } 0 \leq t \leq T \left(N_d + K - \frac{1}{2} \right) \quad (1)$$

$$x(t) = \sum_{p=0}^{N_s-1} \sum_{q=0}^{N_d-1} \left[R_{p,q} g(t-qT) + j I_{p,q} g\left(t-qT - \frac{T}{2}\right) \right] e^{j\theta_{p,q}} \text{ for } qT \leq t \leq (q+K+0.5)T \quad (2)$$

There are N_s sub-carriers in each symbol, N_d is number of data blocks, $D_{p,q}$ is the p^{th} subcarrier of q^{th} QAM symbol, $g(t)$ is response of prototype filter, symbol duration is T , overlapping factor is K , real part of $D_{p,q}$ is $R_{p,q}$, imaginary part of $D_{p,q}$ is $I_{p,q}$ and phase term is

$$\theta_{p,q} = p \cdot \left(\frac{2\pi t}{T} + \frac{\pi}{2} \right)$$

The FBMC/OQAM system has SFB and AFB, which are situated on the transmitter and reception ends, respectively. The SFB and AFB exhibit complementarity and adhere to the Nyquist condition. The frequency spreading (FS)-FBMC necessitates an IFFT/FFT length of KT , where as the Polyphase Network (PPN)-FBMC demands an IFFT/FFT length of N . The building of a PPN filter entails a lower level of CC in comparison to FS-FBMC. A filter bank based on the PPN is constructed by modifying the frequency domain response of the prototype filter (PF) using increments of $1/N$, where N is the number of filters. The PPN filters have a linear phase characteristic and their length is determined by the number of sub-carriers. As the quantity of sub-carriers rises, the complexity of the filter design will also increase. To construct a vector of length KT on the transmitter side, the output of each IFFT block is replicated K times. The vector undergoes filtration via the PF. The addition of the real and imaginary components is achieved by superimposing the imaginary part, as seen in Figure 2. The sequence is thereafter multiplied by the phase term $\Theta_{p,q}$ and afterwards transmitted [37].

Figure 3 illustrates the overlapping configuration of the FBMC/OQAM signal. Each data block signal of two components, separated by $T/2$. Furthermore, the length of one data block is $(K+0.5)T$. The length of M data block is $(K+M-0.5)T$.

The complex input symbols $D_{p,q}$ are converted to real symbols, which composed of real parts ($R_{p,q}$) and imaginary parts ($I_{p,q}$). A phase rotation factors ($\delta_{p,q}$; $\sigma_{p,q}$) given in equation (30 and (4) are multiplied by the resulting symbols to produce an alternate sequence of symbols [38]. By separating the imaginary component by half a symbol period, it is possible to maintain orthogonality between adjacent symbols.

$$\delta_{p,q} = \begin{cases} j \text{ or } -j & \text{for } p = \text{odd} \\ 1 \text{ or } -1 & \text{for } p = \text{even} \end{cases} \quad (3)$$

$$\sigma_{p,q} = \begin{cases} j \text{ or } -j & \text{for } p = \text{even} \\ 1 \text{ or } -1 & \text{for } p = \text{odd} \end{cases} \quad (4)$$

The impulse response of the filter is given in equation (5),

$$g(t) = 1 + 2 \sum_{n=1}^{K-1} G_n \cos\left(\frac{2\pi n t}{KT}\right) \quad (5)$$

The length of the impulse response is KT and number of filter coefficients are $2n-1$. The PAPR of every FBMC symbol is determined as follows and given in equation (6) and (7),

$$PAPR = \frac{\max_{(q-1)T \leq t \leq qT} |x(t)|^2}{E[|x(t)|^2]}; q = 0 \text{ to } N-1 \quad (6)$$

$$PAPR_{dB} = 10 \log_{10} \left(\frac{\max_{(q-1)T \leq t \leq qT} |x(t)|^2}{E[|x(t)|^2]} \right); q = 0 \text{ to } N-1 \quad (7)$$

Here $E[|x(t)|^2]$ is the expected value of FBMC transmitted symbol. The use of the complementary cumulative distribution function (CCDF) is employed for the assessment of PAPR performance. The term "probability" refers to the likelihood that the PAPR would above a specified threshold denoted as $PAPR_0$. The variable $PAPR_0$ is a random variable, where lower values are indicative of superior performance.

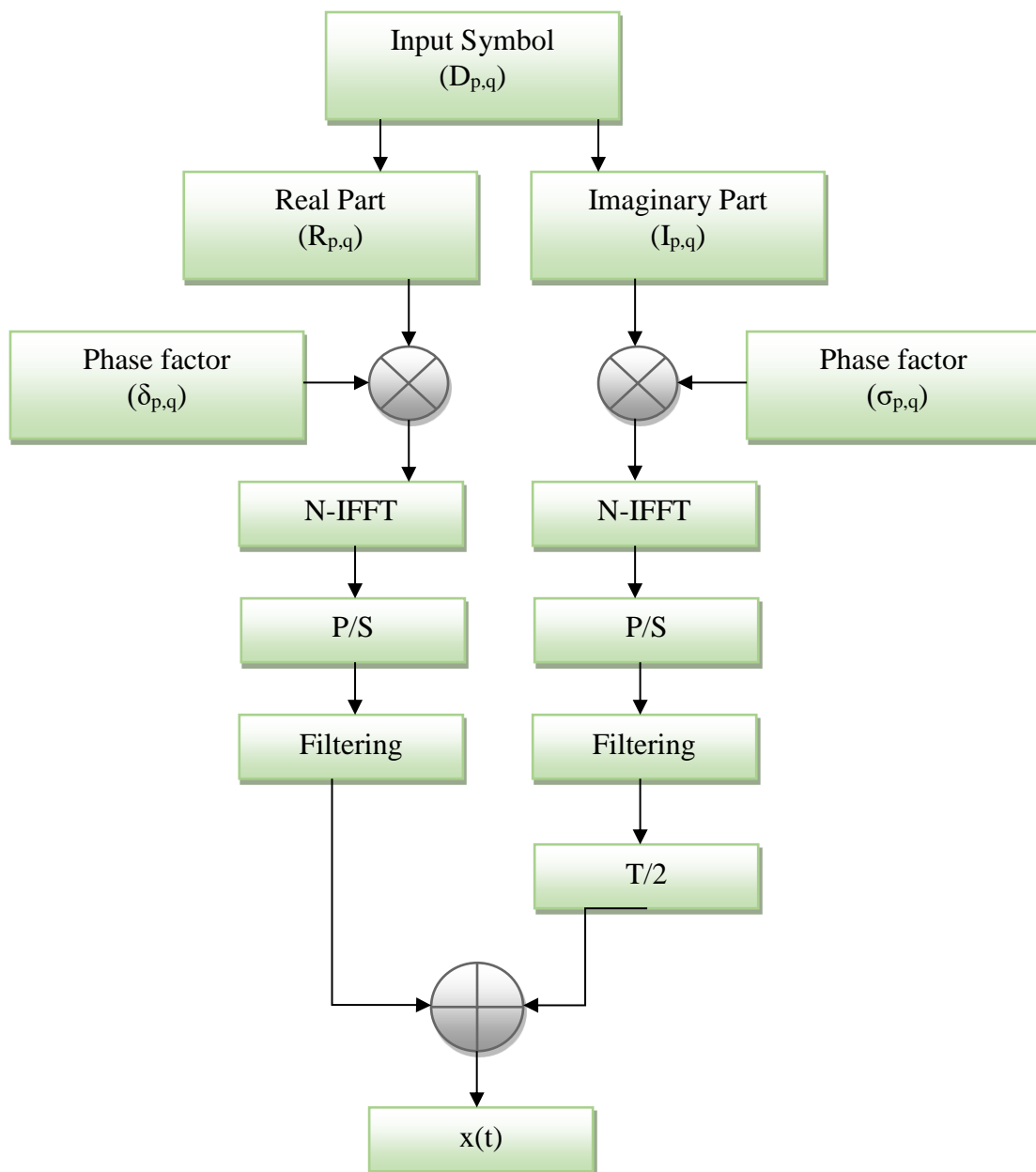


Figure 2. FBMC/OQAM Transmitter Architecture

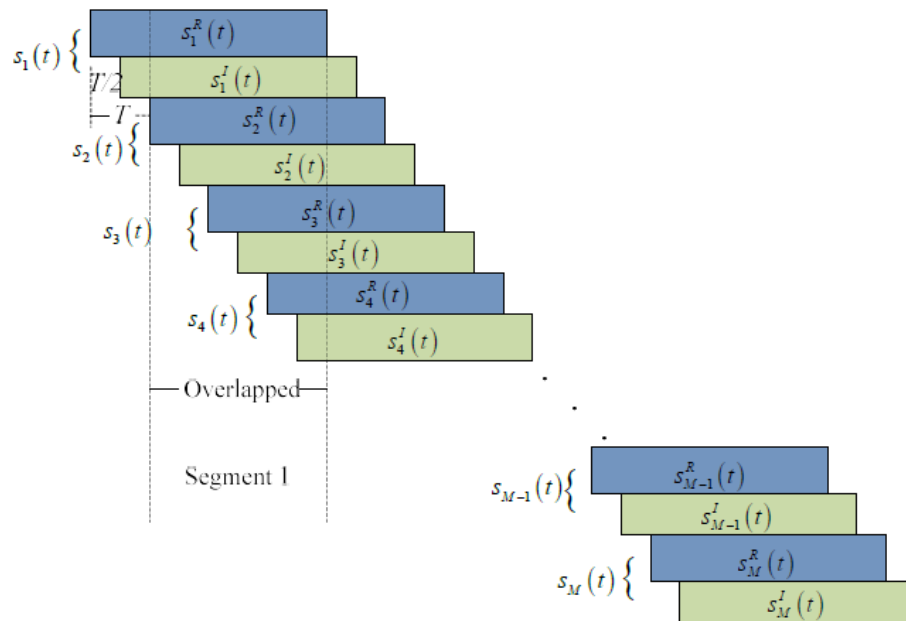


Figure 3. Overlapping signal arrangement

Advantages of FBMC with OQAM:

- Spectral Efficiency:** Cyclic prefix not required and hence better bandwidth utilization.
- Low OoB Emissions:** The prototype filter ensures that the subcarriers have minimal spectral leakage.
- Robustness to Channel Effects:** FBMC is less sensitive to channel effects compared to OFDM.
- Flexibility:** Particularly suitable for applications which employ non-contiguous spectrum allocations.

3.2 GDFT Spreading

A generalization of the Discrete Fourier Transform (DFT) that adds flexibility in signal spreading and allows for enhanced signal shaping, interference management, and robustness. GDFT spreading can be incorporated in FBMC systems to further enhance the system's ability to manage interference and improve spectral efficiency. GDFT enables additional degrees of freedom, providing adaptability in signal design for various channel conditions and application requirements. GDFT spreading is a promising enhancement for FBMC systems, offering significant benefits in spectral efficiency, interference management, and system robustness. While it introduces some implementation challenges, advancements in signal processing and hardware efficiency make GDFT an attractive option for next-generation communication systems, particularly in 6G scenarios.

The complex input data $D_{p,q}$ is split into real ($R_{p,q}$) and imaginary ($I_{p,q}$) parts as represented in equation (8). The real components $R_{p,q}$ is multiplied by the (PRF) phase rotation factor ($\delta_{p,q}$) of the upper IFFT

and the imaginary part $I_{p,q}$ is multiplied by the PRF ($\sigma_{p,q}$) of the lower IFFT. The PRF values are chosen in order to ensure the DFTS produces the lowest PAPR value.

$$D_{p,q} = R_{p,q} + jI_{p,q} \quad (8)$$

Equation (9) and (10) represents the required phase rotation factor patterns, for all the GDFTS methods.

$$\delta_{p,q} = j^{p+2q} \quad (9)$$

$$\sigma_{p,q} = j(-1)^q (-j)^p \quad (10)$$

The DFTS FBMC/OQAM signal is expressed in equation (11) as

$$x(t) = \sum_{p=0}^{N_p-1} \sum_{q=0}^{N_q-1} (-1)^q \left[R_{p,q} g(t-qT) + jI_{p,q} g(t-qT - \frac{T}{2}) \right] e^{j2\pi p \left(t + \frac{T}{4} \right)} \quad (11)$$

3.3 PTS

PTS is a PAPR reduction technique commonly used in MCM systems. The primary goal of PTS is to minimize PAPR by combining multiple phase-shifted versions of subcarrier blocks optimally. FBMC is a highly spectral-efficient system due to its use of overlapping subcarriers with narrowband filters. FBMC lacks a cyclic prefix, making it inherently more prone to distortion caused by high PAPR. High PAPR can degrade system performance by causing nonlinear distortions in the power amplifier, leading to out-of-band emissions and reduced signal quality. The input data block is divided into smaller, disjoint subblocks (called partitions). Each subblock is modulated, and an IFFT operation is applied to generate the corresponding time-domain signal. A set of phase rotation factors is applied to each subblock, and the subblocks are combined. The combination resulting

in the minimum PAPR is selected as the transmitted signal.

The frequency domain of input signal is represented X . This input block X is partitioned into V sub-blocks with $X_m^V = [X_1^V, X_2^V, \dots, X_m^V]^T$. Each sub-block is zero-padded to produce an N -dimensional vector. In the PTS technique, PRF is independently applied to each sub-block. The computing complexity is greatly increased, since IFFT is performed independently for each sub-block. An appropriate complex phase factor is multiplied by each partitioned sub-block. The sequence of optimized phase rotation factor is $r = [r^1, r^2, r^3, \dots, r^V]$,

$$\text{where } r^v = e^{\frac{j2\pi v}{l}}; v = 1 \text{ to } l.$$

The resulting time-domain signal is expressed in equation (12) as

$$X_m(t) = \sum_{v=1}^V r^v x_m^v(t) \quad (12)$$

where, $x_m^v(t)$ is a partial transmit signal.

To get the minimal PAPR value, the phase vector is set as follows and given in equation (13),

$$\begin{bmatrix} r^1, r^2, \dots, r^V \end{bmatrix} = \arg \min_{[r^1, r^2, \dots, r^V]} \max_{0 \leq t \leq T} \left| \sum_{v=1}^V r^v x_m^v \right|^2 \quad (13)$$

The resultant time-domain signal with the lowest PAPR vector can be obtained as given in equation (14),

$$X_m^{\square}(t) = \sum_{v=1}^V b^v x_m^v \quad (14)$$

The presence of a collective of components serves to restrict the range of possible phase variables and thereby reduces the overall complexity of the search process. Within the context of the PTS, the phase rotation operation is implemented on a per-transmit data block signal basis. The application of this approach to individual FBMC symbols yields unsatisfactory results. The optimization performance in FBMC/OQAM systems is negatively affected by the presence of an overlapping structure while using the PTS strategy to reduce PAPR. The basic structure of the PTS is shown in figure 4.

3.4 GDFT spreading with PTS

The integration of GDFT spreading with PTS in FBMC systems provides a very powerful framework for next-generation communication systems. GDFT improves spectral shaping and robustness, while PTS ensures efficient power utilization by reducing PAPR. Although it does pose some computational challenges, it holds great promise for advanced communication scenarios such as 6G and massive IoT deployments.

This opens up a new approach, which is the presentation of a hybrid GDFT and PTS for FBMC/OQAM systems. This novel approach provides a better consideration for overlapping signals, which is an enhancement over the standard GDFT-PTS hybrid approaches. The data are first processed using the GDFT approach. Following this, the signal for the initial PAPR minimization will be obtained. The signal in the frequency domain will be transformed into time, after which the data signal will be sent with the use of the PTS technique.

Segmentation of the data block signal will be either based on an overlap factor. The optimization of the starting data block in each segment involves the multiplication of the phase rotation factor by a certain number of sub-blocks. The determination of the appropriate PRF during the processing of the second data block involves selecting the smallest power value between the first and second data blocks.

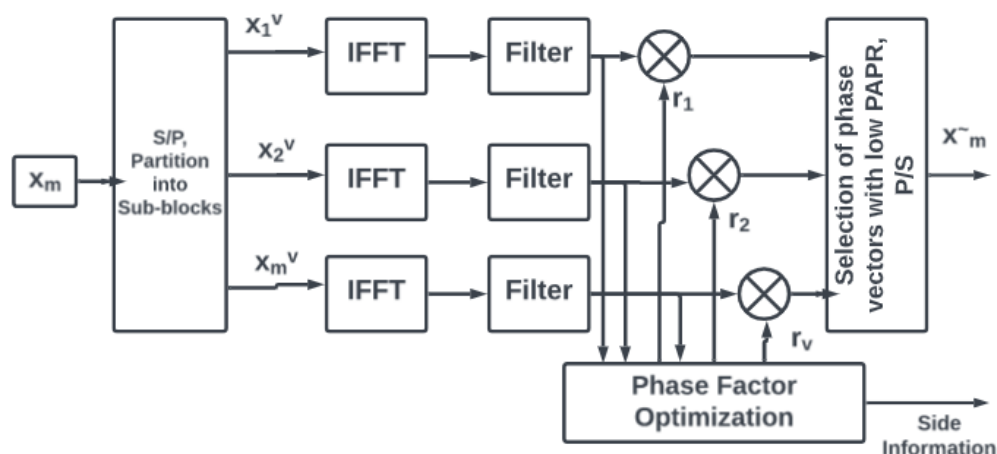


Figure 4. Block Diagram of PTS

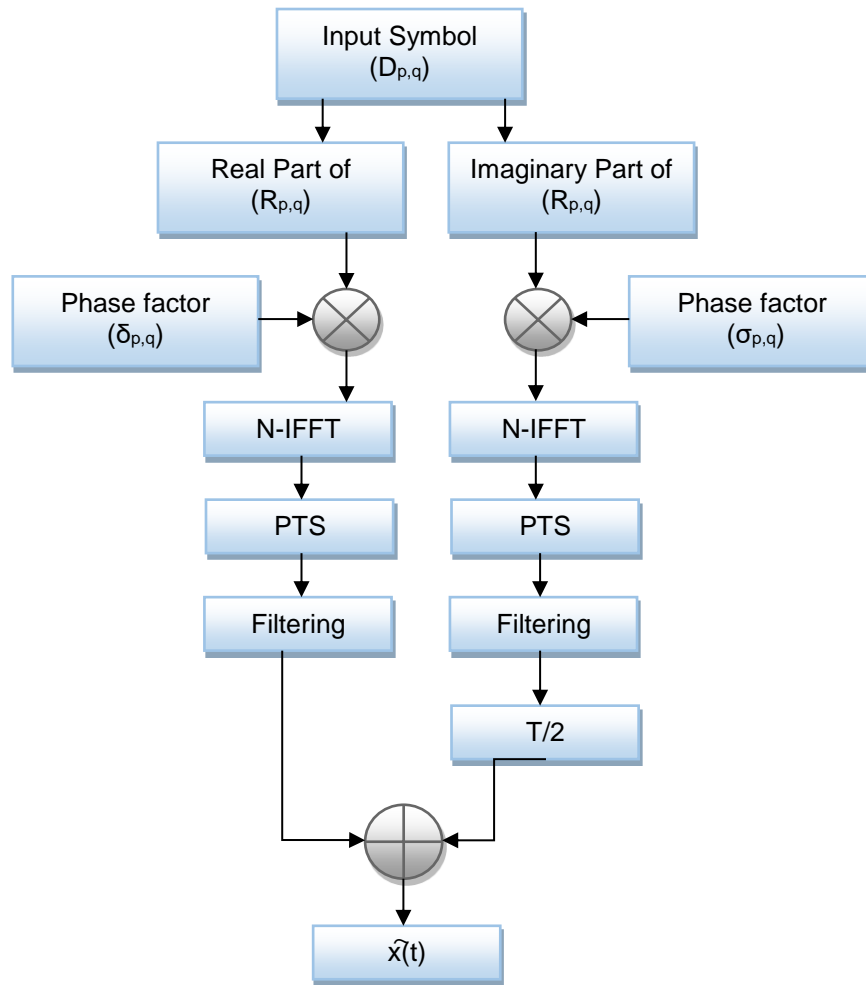


Figure 5. Proposed System

The PTS operation is performed independently on the in-phase and quadrature components of the FBMC, as seen in Figure 5. The resulting sequence is partitioned into V consecutive sub-blocks. These sub-blocks are then extended with zeros to create vectors of length N . This extension is performed after multiplying both the real and imaginary components of the sequence with the corresponding phase patterns $\delta_{p,q}$ and $\sigma_{p,q}$. In order to achieve a low PAPR, the vectors undergo oversampling by the addition of $N(M-1)$ zero values. The oversampling factor, denoted as M , must be greater than or equal to 4 ($M \geq 4$). The optimization procedure is executed in a sequential manner for each individual component in the following manner:

- 1 Consider $k=2\pi\{-1,1\}$ as a phase factor, the total number of candidates are 2^V .
- 2 Utilize PTS method when considering overlapping effects. The output is K times copied before being filtered using the PPN filter.
- 3 Now calculate the PAPR of the filtered sequences. The PAPR of the real part is represented in equation (15).

$$PAPR_R = \frac{\max_{T(q-1)+1 \leq t \leq T(n+q+1)} |\text{Real}(x(t))|^2}{E[|x(t)|^2]} \quad (15)$$

The PAPR of the imaginary part is represented in equation (16).

$$PAPR_I = \frac{\max_{T(q-\frac{1}{2})+1 \leq t \leq T(n+q+\frac{3}{2})} |\text{Imag}(x(t))|^2}{E[|x(t)|^2]} \quad (16)$$

- 4 The real and imaginary parts of optimal phase factors are given in equation (17) and (18),

$$[r^{1,R}, r^{2,R}, \dots, r^{V,R}]_R = \arg \min_{[r^1, r^2, \dots, r^V]} \max_{T(q-1)+1 \leq t \leq T(n+q+1)} \left| \sum_{v=1}^V r^{v,R} x_q^{v,R} \right|^2 \quad (17)$$

$$[r^{1,I}, r^{2,I}, \dots, r^{V,I}]_I = \arg \min_{[r^1, r^2, \dots, r^V]} \max_{T(q-\frac{1}{2})+1 \leq t \leq T(n+q+\frac{3}{2})} \left| \sum_{v=1}^V r^{v,I} x_q^{v,I} \right|^2 \quad (18)$$

- 5 After selecting the candidate with the lowest PAPR, the real and imaginary components are mixed after the latter is separated by $T/2$.

4. Simulation Results

The simulation parameters are given in Table 2. The simulation results are generated using MATLAB. The simulations are provided in this section for verifying the analysis. The performance of the suggested technique is compared with PTS and DFT-S. As compared to these method proposed method provides better results.

Table 2. Simulation Parameters

Parameter	Value
No. of subcarriers (N_s)	128
No. of data blocks (N_d)	10^5
Channel	AWGN, Rician, Rayleigh fading
Modulation	4,16,64-QAM, OQAM
Overlapping factor (K)	4
Oversampling factor (M)	4
Sub-block partition (V)	2, 4
Phase rotation factor	1, -1, -j, j
Prototype filter	PHYDYAS
phase factor	1, -1
FFT length	1024

4.1 PAPR Performance

PAPR is a critical performance metric in FBMC with OQAM. A high PAPR requires a linear and efficient power amplifier, which is challenging to achieve, especially in power-constrained systems. Understanding and analyzing the PAPR performance of FBMC/OQAM is essential to evaluate its feasibility for practical applications. BMC subcarriers overlap in the time-frequency domain but are orthogonal due to the well-designed prototype filters. This overlap can cause high PAPR. The choice of the prototype filter impacts the time-domain envelope of the FBMC signal, indirectly affecting the PAPR.

Figure 6 represents the PAPR analysis for various channels. The performance of PAPR in wireless communication systems varies across different channel types like AWGN, Rician, and Rayleigh due to their distinct fading characteristics. AWGN channels provide better PAPR performance because they do not introduce fading or amplitude fluctuations to the signal. In contrast, Rician and Rayleigh channels, with their multipath effects, distort the signal's amplitude envelope, causing greater variability and higher PAPR in the received signal.

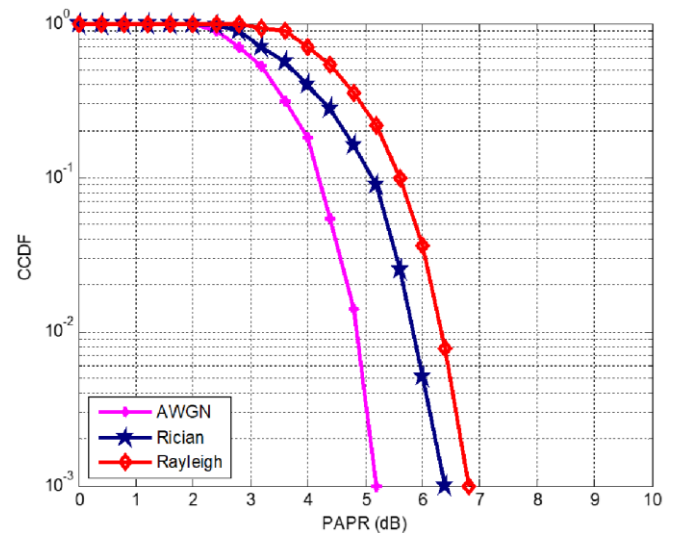


Figure 6. PAPR Analysis for Various Channels

The PAPR analysis for various QAM signals is shown in figure 7. OQAM provides better PAPR performance compared to conventional QAM due to the structural and functional differences in how these modulation schemes handle signal overlap and time-frequency localization, due to the time-offset nature of its modulation, which minimizes peak coincidence between the in-phase and quadrature components. This makes OQAM a preferred choice in scenarios where PAPR reduction and spectral efficiency are critical. Figure 7 shows the PAPR values for different QAM values. Lower QAM signals provides better PAPR values.

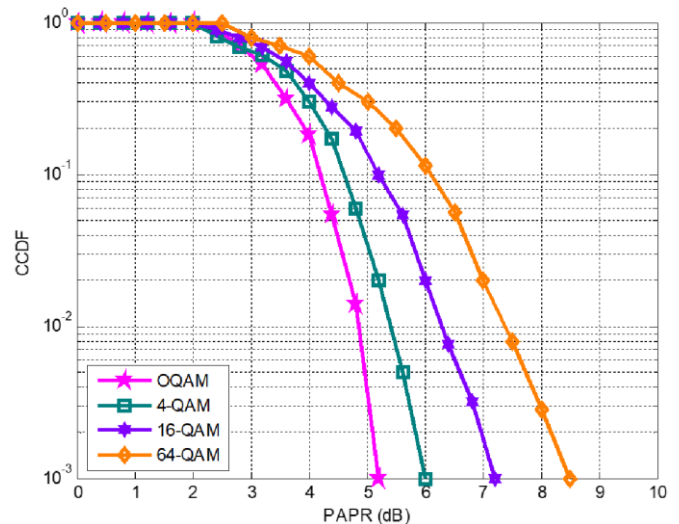


Figure 7. PAPR Analysis for Various QAM signals

Figure 8 shows the PAPR comparison of proposed method with various techniques. The PAPR of the original signal is very high 11.53 dB at a CCDF of 10^{-3} . By applying the various methods the PAPR value reduced. For SLM, DFT spreading, PTS, combining SLM with PTS and combining GDFT with PTS the PAPR is approximately 8.9 dB, 8.1 dB, 7.2 dB, 6.1 dB and 5.2 dB, respectively. The proposed method is better than the other methods in terms of PAPR performance and provides lower PAPR.

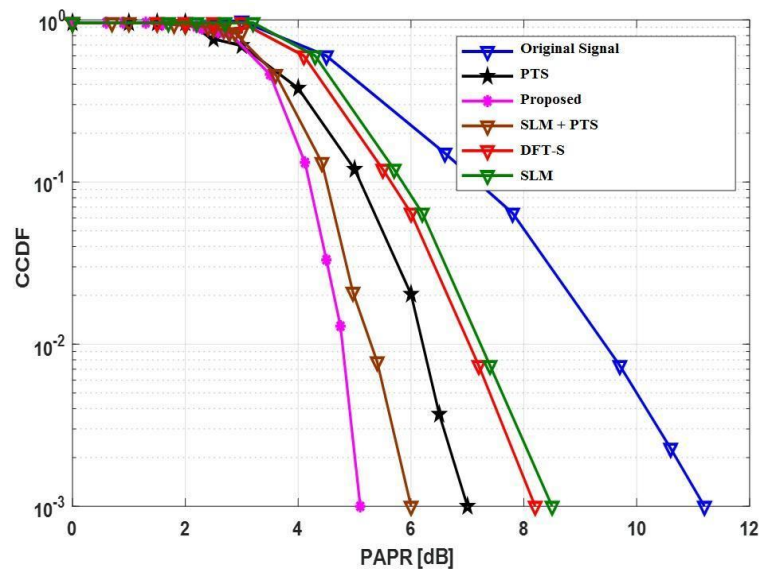


Figure 8. CCDF-PAPR

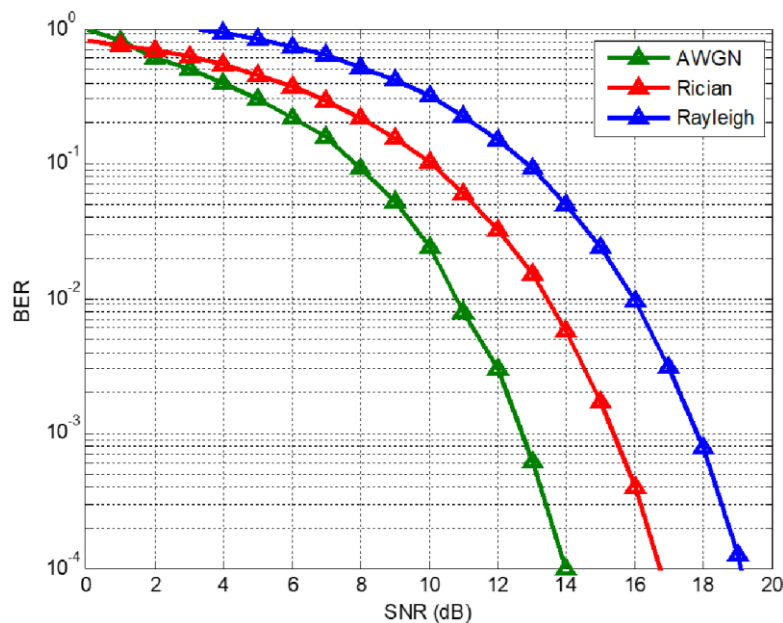


Figure 9. BER Performance of Various Channels

4.2 BER Performance

The ratio of incorrectly received bits to the total transmitted bits. It is a key metric for evaluating the reliability of a communication system. In FBMC systems, BER performance is influenced by factors like channel conditions, noise, interference, and the signal processing techniques employed. The BER performance of FBMC systems depends on multiple factors, including filter design, equalization techniques, modulation schemes, and channel conditions. While challenges such as the absence of a cyclic prefix and PAPR exist, advancements in signal processing techniques and adaptive algorithms ensure that FBMC systems can achieve excellent BER performance, making them suitable for next-generation communication systems like 6G and IoT.

Figure 9 shows the BER performance of various channels. The BER performance of a communication

system depends heavily on the characteristics of the propagation channel. AWGN channels typically provide better BER performance compared to Rician and Rayleigh channels, because they lack the multipath fading effects that cause amplitude and phase distortions. In an AWGN channel, the signal is only affected by additive white Gaussian noise, which is statistically independent of the signal and does not alter its amplitude or phase. This means that the transmitted signal retains its original characteristics apart from the added noise. The stability of the signal in AWGN channels ensures a more consistent SNR, leading to lower error rates. In contrast, fading channels require additional measures to mitigate their impact, which increases complexity and still results in higher BER than in an AWGN environment.

Table 3. PAPR Analysis

Aspects		PAPR (dB)
Modulation Signals	4 - QAM	6
	16 - QAM	7.2
	64 - QAM	8.6
	OQAM	5.2
Channels	AWGN	5.2
	Rician	6.3
	Rayleigh	6.9
Various Methods	Original Signal	11.5
	PTS	7.2
	DFT-S	8.1
	Proposed	5.2

Figure 10 represents the BER performance of various QAM values. OQAM provides better BER performance compared to conventional QAM in specific scenarios due to its improved time-frequency localization, reduced ISI, and resilience to channel distortions. These advantages make OQAM especially suitable for applications in multipath or frequency-selective environments, where achieving low BER is critical.

The BER performance curve shown in the figure 11. The BER is an effective parameter to analyze the impact of the PAPR reduction technique on transmitted data. Several PAPR minimization approaches are effective at lowering the PAPR, but there may be a distortion in signal, due to this system performance reduces. For the SNR of 10 dB, the BER of original signal, SLM, PTS, DFT spreading and proposed system is approximately 0.22, 0.08, 0.045, 0.03 and 0.021, respectively.

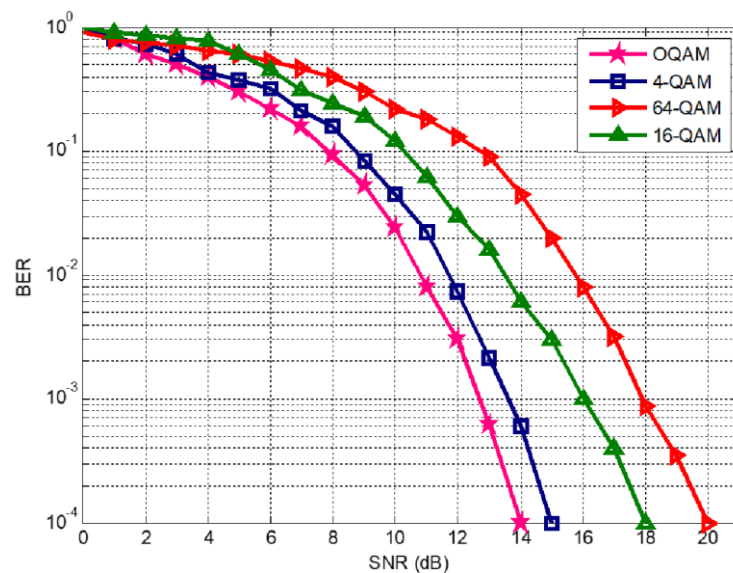
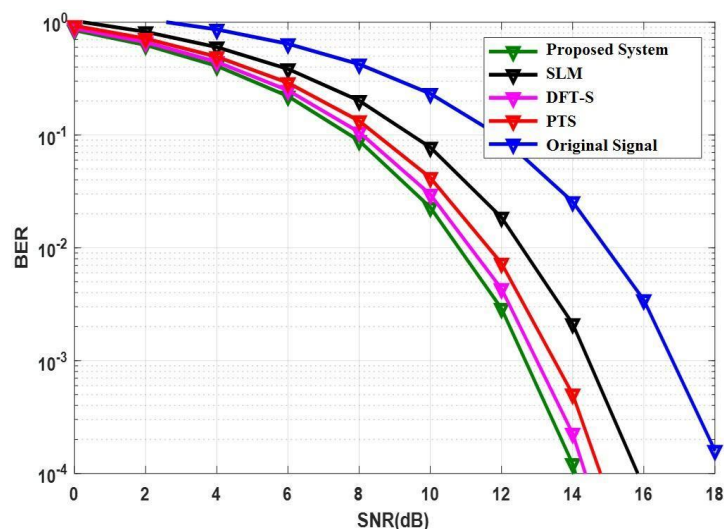
**Figure 10.** BER Performance of Various QAM values**Figure 11.** BER Performance

Table 4. BER values at different conditions

Aspects		BER at SNR = 10 dB
Modulation Signals	4 - QAM	4.3×10^{-2}
	16 - QAM	1.2×10^{-1}
	64 - QAM	2.2×10^{-1}
	OQAM	2.1×10^{-2}
Channels	AWGN	2.1×10^{-2}
	Rician	1×10^{-1}
	Rayleigh	3×10^{-1}
Various Methods	Original Signal	2.2×10^{-1}
	PTS	4.5×10^{-2}
	DFT-S	3×10^{-2}
	Proposed	2.1×10^{-2}
	SLM	8×10^{-2}

4.3 Spectral Efficiency Performance

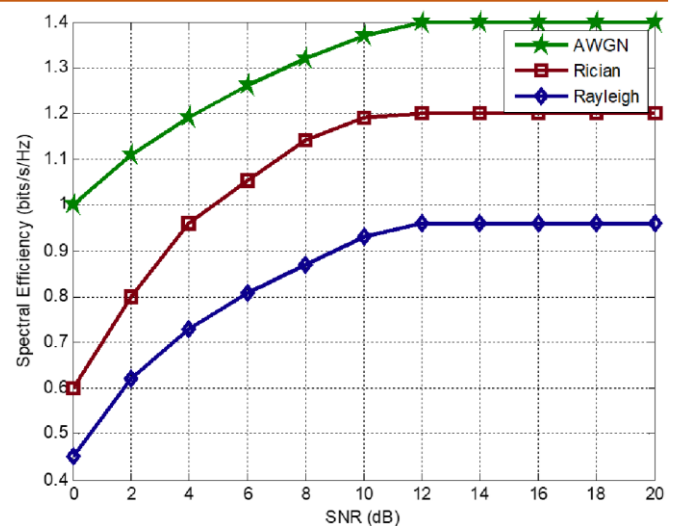
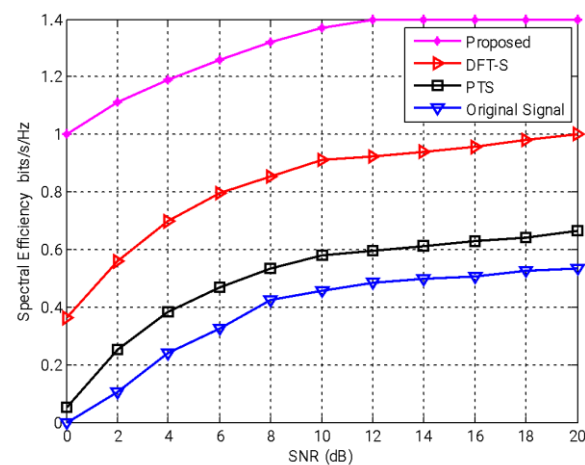
Spectral efficiency is a critical performance metric in communication systems, representing the amount of data transmitted per unit bandwidth per unit time. In systems, spectral efficiency is typically better than in traditional OFDM systems due to their unique features. The excellent frequency confinement of FBMC subcarriers allows for asynchronous multi-user communication without significant interference. This makes FBMC particularly efficient in scenarios like uplink transmissions in 5G and beyond, where users may not be perfectly synchronized. This asynchronous capability avoids guard bands and timing synchronization overhead, improving spectral efficiency. The spectral efficiency of an FBMC system also depends on the design of its prototype filter. A well-optimized filter maximizes spectral confinement while maintaining the required signal fidelity and robustness against ISI and ICI.

The spectral efficiency is given by

$$SE = C_r k(1-B)E_T E_F$$

$$SE = \frac{C_r k(1-B)T_i S_d}{(T_i + T_t)S_t}$$

where channel coding rate is C_r , k indicates number of bits per subcarrier, T_i is information transmission length, T_t transmission tail length, B is BER, S_d is information-carrying subcarriers and S_t is total no. of subcarriers.

**Figure 12.** Spectral Efficiency at Various Channels**Figure 13.** SNR vs SE

The spectral efficiency is shown in figure 13. The analysis of a communication system's performance involves the consideration of spectral efficiency as an essential metric. A MATLAB-based simulation is provided for the purpose of conducting spectral efficiency study on FBMC-based MCM approaches. Spectral efficiency is measured by considering the parameters usable bandwidth and total bandwidth. The SE of proposed method is 1.41bits/s/Hz at SNR of 20dB. The SE is 1, 0.69, and 0.58 for DFT-S, PTS and original signal, respectively.

Comparison with Related Studies:

This section clearly compares the current investigation with the relevant research, as outlined in Table 6. This section systematically analyzes our new study with older studies, using all information mentioned in Table 6. The essential assessment metrics and their corresponding measures have been thoroughly examined in previous sections. Table 6 highlights this research's unique advantage in achieving the highest calculated PAPR minimization across all literature addressing PAPR reduction.

Table 5. Spectral Efficiency Values at Different Conditions

Aspects		SE (bits/s/Hz) at SNR = 20dB
Channels	AWGN	1.4
	Rician	1.2
	Rayleigh	0.97
Methods	Original Signal	0.58
	PTS	0.69
	DFT-S	1
	Proposed	1.4

Table 6. Compares the proposed research with the existing work, highlighting different approaches for minimizing PAPR in FBMC

Author & Year	Reference	Techniques	PAPR (dB)
Moon <i>et al.</i> , [2018]	[24]	SBO	6.6
Van Der Neut <i>et al.</i> , [2014]	[25]	ACE-SGP	7.3
Sidiq <i>et al.</i> , [2021]	[26]	Hybrid SLM-PTS	5.6
Jirajaracheep <i>et al.</i> , [2020]	[27]	Trellis-based D-SLM	8.4
		Trellis-based D-SLM with ABC	8.6
Li <i>et al.</i> , [2022]	[28]	PTS-DPSO-TH	6.23
Hu <i>et al.</i> , [2022]	[29]	CUPSO-PTS	6.2
		BPSO-PTS	6.4
Lv <i>et al.</i> , [2020]	[30]	GA-BPTS	10.2
Rajendra Prasad <i>et al.</i> , [2022]	[31]	PSO-JPTS	7.4
Necmi Taşpınar <i>et al.</i> , [2019]	[32]	DSO-PTS	6.67
Boudjelkha <i>et al.</i> , [2023]	[33]	RCF	5.6
Sinha <i>et al.</i> , [2023]	[34]	TR and clipping	8.94
Vuppula Manohar <i>et.al</i> , [2024]	[35]	DEHOA	6.42
Proposed	-	Hybrid MGDFT-PTS	5.2

5. Conclusions

In this article, we investigated the performance of the FBMC/OQAM system using a hybrid approach that combines the MGDFT and PTS techniques, with a focus on addressing the challenges of 5G/6G communication systems. The primary performance metrics evaluated include BER, SE, and PAPR. Our results demonstrate that the proposed hybrid MGDFT-PTS approach significantly reduces PAPR compared to conventional FBMC/OQAM systems while maintaining acceptable BER performance. Furthermore, the integration of MGDFT enhances spectral efficiency by effectively reducing OoB emissions. These

improvements make the proposed technique highly suitable for 5G/6G networks, which demand high spectral efficiency and reliable transmission with minimal power fluctuations. By offering a balanced trade-off between PAPR reduction, BER performance, and spectral efficiency, the hybrid MGDFT-PTS approach proves to be a promising solution for future 5G/6G communication systems. Future research can explore the scalability and adaptability of this method to meet diverse 5G/6G scenarios and channel conditions.

6. Future Directions

The promising results obtained from the hybrid MGDFT-PTS approach in enhancing the performance of FBMC/OQAM systems motivate further investigations to fully exploit its potential in next-generation wireless networks, particularly 6G. Several future research directions can be explored to extend this study. The future studies can focus on evaluating the robustness of the proposed hybrid approach under varying channel conditions, including high mobility scenarios and harsh fading environments typical of 6G networks. Leveraging machine learning techniques to dynamically optimize the PTS parameters and MGDFT coefficients can further improve performance and reduce computational complexity. By developing low-complexity algorithms for the hybrid MGDFT-PTS method will be crucial to make it feasible for real-time applications in 6G communication systems. By extending the proposed technique to work efficiently with massive MIMO configurations and cooperative networks would enhance its applicability in ultra-dense 6G environments. While investigating energy-efficient designs and power optimization techniques will be essential to minimize the power consumption associated with hybrid processing while maintaining system performance.

References

- [1] K.K. Vaigandla, (2022). Communication technologies and challenges on 6G networks for the Internet: Internet of Things (IoT) based analysis. In 2022 2nd International Conference on Innovative Practices in Technology and Management (ICIPTM), 2, 27-31. IEEE. <https://doi.org/10.1109/ICIPTM54933.2022.9753990>
- [2] W. Khrouf, M. Siala, F. Abdelkefi, How much FBMC/OQAM is better than FBMC/QAM? A tentative response using the POPS paradigm. Wireless Communications and Mobile Computing, 2018(1), (2018) 4637181. <https://doi.org/10.1155/2018/4637181>
- [3] K.K. Vaigandla, J. Benita, Novel Algorithm for Nonlinear Distortion Reduction Based on Clipping and Compressive Sensing in OFDM/OQAM System. International Journal of Electrical and Electronics Research, 10(3), (2022) 620-626. <https://doi.org/10.37391/IJEER.100334>
- [4] Y. Xia, J. Ji, Low-Complexity Blind Selected Mapping Scheme for Peak-to-Average Power Ratio Reduction in Orthogonal Frequency-Division Multiplexing Systems. Information, 9(9), (2018) 220. <https://doi.org/10.3390/info9090220>
- [5] K.K. Vaigandla, J. Benita, Study and Analysis of Various PAPR Minimization Methods. International Journal of Early Childhood Special Education, 14(3), (2022) 1731-1740. <http://doi.org/10.9756/INT-JECSE/V14I1.221001>
- [6] K.K. Vaigandla, J. Benita, A Novel PAPR Reduction in Filter Bank Multi-Carrier (FBMC) with Offset Quadrature Amplitude Modulation (OQAM) Based VLC Systems. International Journal on Recent and Innovation Trends in Computing and Communication, 11(5), (2023) 288-299. <https://doi.org/10.17762/ijritcc.v11i5.6616>
- [7] S. Lu, D. Qu, Y. He, Sliding window tone reservation technique for the peak-to-average power ratio reduction of FBMC-OQAM signals. IEEE Wireless Communications Letters, 1(4), (2012) 268-271. <https://doi.org/10.1109/WCL.2012.062512.120360>
- [8] Z. Kollár, P. Horváth, PAPR reduction of FBMC by clipping and its iterative compensation. Journal of Computer Networks and Communications, (1), (2012) 382736. <https://doi.org/10.1155/2012/382736>
- [9] Z. Kollar, L. Varga, K. Czimer, (2012). Clipping-based iterative PAPR-reduction techniques for FBMC. In OFDM 2012; 17th International OFDM Workshop 2012 (InOWo'12) (pp. 1-7). VDE.
- [10] M. Laabidi, R. Zayani, R. Bouallegue, (2015). A novel multi-block selective mapping scheme for PAPR reduction in FBMC/OQAM systems. In 2015 World Congress on Information Technology and Computer Applications (WCITCA) (pp. 1-5). IEEE. <https://doi.org/10.1109/WCITCA.2015.7367014>
- [11] S.K.C. Bulusu, H. Shaiek, D. Roviras, Reducing the PAPR in FBMC-OQAM systems with low-latency trellis-based SLM technique. EURASIP Journal on Advances in Signal Processing, (2016), 132. <https://doi.org/10.1186/s13634-016-0429-9>
- [12] P. Jirajaracheep, S. Sanpan, P. Boonsrimuang, P. Boonsrimuang, (2018). PAPR reduction in FBMC-OQAM signals with half complexity of trellis-based SLM. In 2018 20th International Conference on Advanced Communication Technology (ICACT) (pp. 1-5). IEEE. <https://doi.org/10.23919/ICACT.2018.8323624>
- [13] Y. Zhou, T. Jiang, C. Huang, S. Cui, (2013). Peak-to-average power ratio reduction for OFDM/OQAM signals via alternative-signal method. IEEE Transactions on Vehicular Technology, 63(1), 494-499. <https://doi.org/10.1109/TVT.2013.2273557>
- [14] C. Ye, Z. Li, T. Jiang, C. Ni, Q. Qi, PAPR reduction of OQAM-OFDM signals using segmental PTS scheme with low complexity. IEEE Transactions on Broadcasting, 60(1), (2013) 141-147. <https://doi.org/10.1109/TBC.2013.2282732>
- [15] J.H. Moon, Y.R. Nam, J.H. Kim, PAPR Reduction in the FBMC-OQAM System via Segment-Based

- Optimization. IEEE Access, 6, (2018) 4994–5002.
<https://doi.org/10.1109/ACCESS.2018.2794366>
- [16] T. Jiang, C. Ni, C. Ye, Y. Wu, K. Luo, A Novel Multi-Block Tone Reservation Scheme for PAPR Reduction in OQAM-OFDM Systems. IEEE Transaction on Broadcast. 61(4), (2015) 717–723.
<https://doi.org/10.1109/TBC.2015.2465146>
- [17] K.K Vaigandla, J. Benita, Study and analysis of multi carrier modulation techniques – FBMC and OFDM, Materials Today: Proceedings, 58(1), (2022) 52–56.
<https://doi.org/10.1016/j.matpr.2021.12.584>
- [18] D. J. Na, K. Choi, Low PAPR FBMC. IEEE Transactions on Wireless Communication. 17(1), (2018) 182–193.
<https://doi.org/10.1109/TWC.2017.2764028>
- [19] S. Vangala, S. Anuradha, (2015), Hybrid PAPR reduction scheme with selective mapping and tone reservation for FBMC/OQAM. In Proceedings of the 3rd International Conference on Signal Processing, Communication and Networking, IEEE, Chennai, India, (pp. 1–5).
<https://doi.org/10.1109/ICSCN.2015.7219877>
- [20] R. Gopal, S.K. Patra, (2015), Combining Tone Injection and Companding Techniques for PAPR Reduction of FBMC-OQAM System. In Proceedings of the 2015 Global Conference on Communication Technologies, IEEE, Thuckalay, India, pp.709–713.
<https://doi.org/10.1109/GCCT.2015.7342756>
- [21] J. Zhao, S. Ni, Y. Gong, Peak-to-Average Power Ratio Reduction of FBMC/OQAM Signal Using a Joint Optimization Scheme. IEEE Access 5, (2017) 15810–15819.
<https://doi.org/10.1109/ACCESS.2017.2700078>
- [22] H. Wang, X. Wang, L. Xu, W. Du, Hybrid PAPR Reduction Scheme for FBMC/OQAM Systems Based on Multi Data Block PTS and TR Methods. IEEE Access, 4, (2016) 4761–4768.
<https://doi.org/10.1109/ACCESS.2016.2605008>
- [23] R. Nissel, M. Rupp, Pruned DFT-Spread FBMC: Low PAPR, Low Latency, High Spectral Efficiency. IEEE Transactions on Communications. 66(10), (2018) 4811–4825.
<https://doi.org/10.1109/TCOMM.2018.2837130>
- [24] J.H. Moon, Y.R. Nam, J.H. Kim, PAPR reduction in the FBMC-OQAM system via segment-based optimization, IEEE Access, 6, (2018) 4994–5002.
<https://doi.org/10.1109/ACCESS.2018.2794366>
- [25] N. van der Neut, B.T. Maharaj, F. de Lange, G.J. González, F. Gregorio, J. Cousseau, PAPR reduction in FBMC using an ACE-based linear programming optimization, EURASIP Journal on Advances in Signal Processing, 172, (2014) 1–21.
<https://doi.org/10.1186/1687-6180-2014-172>
- [26] S. Sidiq, J.A., Sheikh, F. Mustafa, B.A., Malik, I.B., Sofi, PAPR minimization of FBMC/OQAM scheme by hybrid SLM and PTS using artificial: bee-Colony phase—Optimization, Arabian Journal for Science and Engineering, 46(10), (2021) 9925–9934.
<https://doi.org/10.1007/s13369-021-05625-4>
- [27] P. Jirajaracheep, T. Mata. P. Boonsrimuang, (2020), PAPR reduction in FBMC-OQAM systems using trellis-based D-SLM with ABC algorithm, 17th International Conference on Electrical Engineering/Electronics, Computer, Telecommunications and Information Technology, IEEE, Phuket, Thailand, 506–509.
<https://doi.org/10.1109/ECTI-CON49241.2020.9158300>
- [28] L. Li, L. Xue, X. Chen, D. Yuan, Partial transmit sequence based on discrete particle swarm optimization with threshold about PAPR reduction in FBMC/OQAM system, IET Communications, 16(2), (2022) 142–150.
<https://doi.org/10.1049/cmu2.12321>
- [29] F. Hu, H. Xu, L. Jin, J. Liu, Z. Xia, G. Zhang, J. Xiao, Continuous-unconstrained and global optimization for PSO-PTS based PAPR reduction of OFDM signals, Physical Communication, 55, (2022) 101825.
<https://doi.org/10.1016/j.phycom.2022.101825>
- [30] S. Lv, J. Zhao, L. Yang, Q. Li, Genetic algorithm based bilayer PTS scheme for peak-to-average power ratio reduction of FBMC/OQAM signal, IEEE Access, 8, (2020) 17945–17955.
<https://doi.org/10.1109/ACCESS.2020.2967846>
- [31] D. Rajendra Prasad, S. Tamil, B. Chourasia, (2021) PAPR Reduction for FBMC-OQAM Signals Using PSO-Based JPTS Scheme, In Innovations in Electronics and Communication Engineering: Proceedings of the 9th ICIECE 2021, Springer, 29–38. https://doi.org/10.1007/978-981-16-8512-5_4
- [32] N. Taşpınar, Ş. Şimşir, Dual symbol optimization-based partial transmit sequence technique for PAPR reduction in WOLA OFDM waveform, International Journal of Communication Systems, 32(14), (2019) e4081.
<https://doi.org/10.1002/dac.4081>
- [33] A. Boudjelkha, A. Khelil, H. Merah, Repeated Clipping Filtering with Nonlinear Companding for PAPR Reduction in MIMO FBMC/OQAM System, International Journal of Intelligent Engineering & Systems, 16(4), (2023) 630–641.
<https://doi.org/10.22266/ijies2023.0831.51>
- [34] H.K. Sinha, A. Saurabh, K. Anand, D. Pradhan. PAPR Detection Using TR and Clipping & Filtering

(CF)-Reduction Technique for 5G Communication System (5G-CS): Comparative Analysis, 5(2), (2023) 1-5.

- [35] V. Manohar, R. Mohandas, K.K. Padakanti, K.K. Vaigandla, Discrete Elephant Herding Optimization Algorithm for Analysis of PAPR, BER and Spectral Efficiency in FBMC/OQAM System. International Research Journal of Multidisciplinary Technovation, 6(5), (2024) 94-109. <https://doi.org/10.54392/irjmt2457>
- [36] K. K. Vaigandla, J. Benita, 'Selective Mapping Scheme Based on Modified Forest Optimization Algorithm for PAPR Reduction in FBMC System'. Journal of Intelligent & Fuzzy Systems, 45(4), (2023) 5367-5381. <https://doi.org/10.3233/JIFS-222090>
- [37] D. Kong, X. Zheng, Y. Yang, Y. Zhang, T. Jiang, A novel DFT-based scheme for PAPR reduction in FBMC/OQAM systems, IEEE Wireless Communications Letters, 10(1), (2020) 161-165. <https://doi.org/10.1109/LWC.2020.3024179>
- [38] S. Sidiq, J.A. Sheikh, F. Mustafa, B.A. Malik, I.B. Sofi, PAPR minimization of FBMC/OQAM scheme by hybrid SLM and PTS using artificial: bee-Colony phase-Optimization, Arabian Journal for Science and Engineering, 46, (2021) 9925-9934. <https://doi.org/10.1007/s13369-021-05625-4>

About the License

© The Author(s) 2025. The text of this article is open access and licensed under a Creative Commons Attribution 4.0 International License.

Authors Contribution Statement

N Sivapriya: Conceptualization, Methodology, Software, Validation, Supervision, Validation. Karthik Kumar Vaigandla: Conceptualization, Visualization, Supervision, Writing - Review & Editing. R. Mohandas: Methodology, Data Curation, Writing - Review & Editing. Kiruba Sankar K: Conceptualization, Formal Analysis, Validation. All the authors read and approved the final version of the manuscript.

Funding

The authors declare that no funds, grants or any other support were received during the preparation of this manuscript.

Competing Interests

The authors declare that there are no conflicts of interest regarding the publication of this manuscript.

Data Availability

The data supporting the findings of this study can be obtained from the corresponding author upon reasonable request.

Has this article screened for similarity?

Yes